A mechanics prediction of the behaviour of mono-crystalline silicon under nano-indentation

T. Vodenitcharova, L.C. Zhang [*]

School of Aerospace, Mechanical and Mechatronic Engineering, The University of Sydney, NSW 2006, Australia

Abstract

This paper uses a new constitutive model developed recently by the authors to analyse the multi-phase transformations in mono-crystalline silicon when subjected to nano-indentation. The finite element method is employed to the integration of the stress–strain relationship. A very good agreement is reached with the experimental measurements, with an accurate prediction of the observed pop-in and pop-out and detailed phase transformation events in loading and unloading. It was found that due to the change of microstructures, the material in the deformation zone could experience a local unloading during indentation loading or undergo a local loading during indentation unloading. The phase transformation events during indentation are closely related to the variation of both the deviatoric and hydrostatic stress components.
© 2003 Elsevier Science Ltd. All rights reserved.

Keywords: Theoretical prediction; Silicon; Phase transformation; Nano-indentation

1. Introduction

Mono-crystalline silicon has been ideal for the investigation of the pressure-induced polymorphism of materials. It has been confirmed both experimentally and theoretically that under certain loading conditions mono-crystalline silicon undergoes brittle-to-ductile solid phase transitions at room temperature. Over the decades, more than 12 stable and metastable solid phases have been observed in pure hydrostatic pressure tests and nano-indentation. Some major transformation events in loading can be briefly summarized as follows: (1) β-tin metallic Si (Si II) at 10–12 GPa leading to a 22% volumetric reduction (Hu et al., 1986); (2) a further denser phase, Imma silicon (Si XI) at 13.2–15.6 GPa (McMahon et al., 1994); (3) a primitive hexagonal (ph, Si V) structure at 14 GPa; (4) Cmca Si (Si VI) above 38 GPa (Hanfland et al., 1999); (5) a hexagonal close-packed structure (hcp, Si VII) at 40–49 GPa (Hu et al., 1986); and (6) the densest microstructure, face-centred cubic (fcc, Si X) at 79 GPa, claimed to be stable up to 248 GPa (Duclos et al., 1990).

Not all the phases are reversible. In unloading, the transition of hcp to ph and then to β-tin has been confirmed (Tolbert et al., 1996). Further depressurisation does not lead to the original diamond cubic Si (Si I). It is thought that β-tin Si transforms through the metastable rhombohedral Si (R8, Si XII) to body centred cubic (bcc, Si III) (Pfrommer et al., 1997; Piltz et al., 1995), or directly to amorphous Si. On the other hand, it has been found that although the phase transformation is pressure-dependent under pure hydrostatic stresses, the deviatoric stresses influence the hydrostatic thresholds (Wu et al., 1999) and a drop in the transition pressure for the transformation from Si I to Si II from 11.3–12.5 to 8.5 GPa was recorded (Hu et al., 1986).

The phase transformations have also been observed in micro/nano-indentations, where the stress state is complex, with both hydrostatic and deviatoric stress components nonzero. The load-penetration curve and the corresponding phase transformations in loading/unloading have been the main interest. Silicon proved to be hysteretic in nature and exhibited plasticity common for metals (Callahan and Morris, 1992; Gogotsi, 2000; Mann and van Heerden, 2000; Swain, 1998; Weppelmann et al., 1993, 1995; Williams et al., 1999; Zarudi and Zhang, 1999). Some observed a distinct displacement discontinuity in loading, called pop-in; but others additionally recorded well-defined transition steps only in unloading, called pop-out.

Metallisation of silicon has been at times attributed to dislocation activity alone, and the pop-ins/outs to a deep lateral crack beneath the indenter. However this has not been experimentally confirmed. At present, it is widely believed that plasticity in indentation is largely caused by phase transformation that is initiated at a high level of deviatoric stresses, but is further facilitated by the presence of a hydrostatic stress (Zhang and Tanaka, 1999). The transition steps in a loading/unloading curve occur when a large volume of material undergoes a solid phase change. In loading, Si I transforms to the denser Si II and thus the displacement discontinuity (pop-in) appears due to a sudden volumetric reduction. In contrast, in unloading the transition is to a lower density structure associated with a volumetric expansion, and consequently, the event of pop-out.

The interesting behaviour of silicon has further attracted the investigations into the applicability of the existing constitutive models by performing FEA for indentation (Yoshino et al., 2001; Zhang and Mahdi, 1996). In their paper, Zhang and Mahdi (1996) investigated the elastic–plastic behaviour of Si using the von Mises model. In loading the load-displacement curve obtained by the FEM simulations is close to the experimental curve; however, in unloading discrepancies are readily observed. The numerical analysis also misses the transition step in unloading (pop-out) and predicts larger plasticity than recorded.

Apart from the above studies, atomistic investigations into the behaviour of silicon using molecular dynamics simulations have also been conducted (Cheong and Zhang, 2000; Inamura and Takezawa, 1997; Zhang and Tanaka, 1999). Zhang and Tanaka (1999) concluded that the large plastic deformation in silicon mono-crystals is induced by amorphous phase transformation, which is initiated in loading by a critical octahedral shear stress of around 4.6 GPa and then further developed by the hydrostatic stress.

The experimental and numerical studies have greatly contributed to the understanding of the microstructural changes of silicon under various stresses. However, a mechanical prediction has been difficult because no fundamental model has been available. Recently, a new constitutive theory was developed for the complex behaviour of silicon (Vodenitcharova and Zhang, submitted for publication), which is capable of describing the multi-phase transformations of a class of brittle materials. The present paper will use this new model to explore mathematically the mechanics associated with the nano-indentation of mono-crystalline silicon.

2. Constitutive model of multi-phase transformation

The constitutive model recently established by Vodenitcharova and Zhang (submitted for publication) was based on the classical incremental theory of plasticity and the experimental observations discussed in
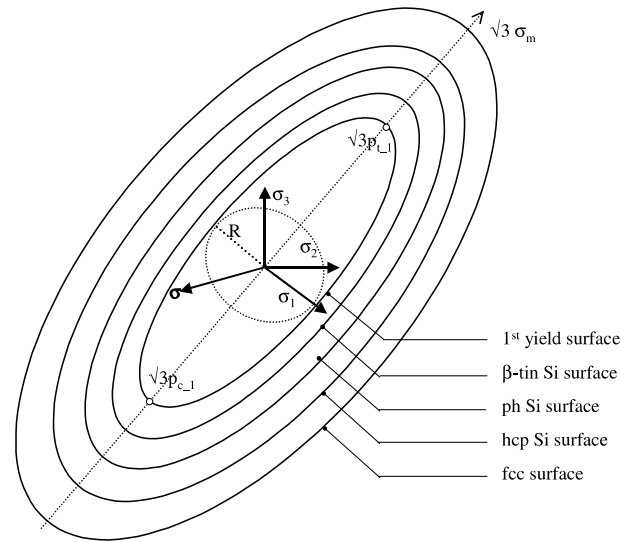
Fig. 1. Yield/phase transformation surfaces in the principal stress space.

Section 1. While the details of the formulation can be found in their paper, the main idea of handling the phase transformations in this model is outlined below.

A set of fixed ellipsoidal surfaces was introduced in the principal stress space (Fig. 1) to mark the onset of plasticity and subsequent phase transformations. At an elevated hydrostatic pressure, for instance, a phase transformation happens when the stress vector $\boldsymbol{\sigma}$ reaches the corresponding phase transformation surface. This phase then develops according to the flow rule and hardening rule until the next surface is reached. Unloading is elastic and is also accompanied by phase changes; thus, additional phase transformation surfaces are introduced (not shown in Fig. 1).

The yield/phase transformation surfaces are assumed symmetric about the π-plane. The material constants are determined by fitting the experimental results (Zarudi and Zhang, 1999). The first yield surface is specified along the isocline of the principal stress space by a hydrostatic threshold $p_{c\_1} = 8.5$ GPa (Fig. 2), and in a perpendicular direction by a yield stress in pure shear $k = 2.5$ GPa, corresponding to an octahedral stress in pure shear $\tau_0 = 2.04$ GPa. After reaching this yield surface silicon becomes elastic–plastic. Then the surface expands isotropically with a tangent bulk modulus $K_1^T = 30$ GPa, as $\Delta R = |\Delta p_c|$. The reason for some plasticity to be allowed in the new model, with no phase change occurring, is that planar defects and dislocations are always observed experimentally in the zone under the transformation zone even at a very small penetration (Zarudi and Zhang, 1999). The depths of their penetration into the substrate can be much greater than the depth of the transformation zone.

The first phase transformation, Si I → Si II (β-tin), occurs at $p_{c\_2} = 10$ GPa. Having specified again that $\Delta R = |\Delta p_c|$ the yield stress in pure shear is calculated as $k = 3.6$ GPa and the octahedral stress in pure shear $\tau_0 = 2.91$ GPa, respectively. When the phase changes, the material consequently reduces its volume by 22% of the total volumetric strain, and then hardens with a tangent bulk modulus of $K_2^T = 1$ GPa. The second phase transformation, β-tin → ph Si is specified by $p_{c\_3} = 16$ GPa and $K_3^T = 1$ GPa. The third transformation ph Si → hcp Si occurs at $p_{c\_4} = 40$ GPa and develops further with $K_4^T = 1$ GPa, and the last transition hcp Si → fcc Si eventuates at $p_{c\_5} = 79$ GPa with $K_5^T = 1$ GPa.

The constitutive model is programmed in FORTRAN77 and implemented as a user-supplied subroutine into the commercially available FEA code, ADINA (ADINA, 1997). The FEA simulations are performed
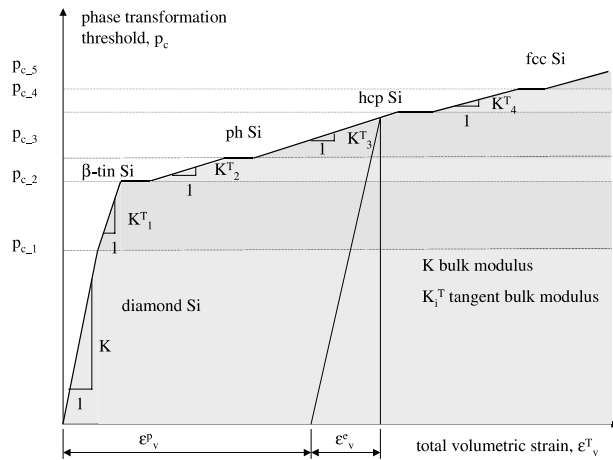
Fig. 2. Phase transformation thresholds in hydrostatic compression.

with a Young's modulus of 80 GPa and a Poisson's ratio of 0.17. These values are within the range reported in the literature (Bever and Wert, 1990) and provided on the web (www.design.caltech.edu/Research/ MEMS/siliconprop.html; www.webelements.com/webelements/elements/t4xt/Si/phys.html).

3. Results and discussion

A 3D finite element model is created using ADINA for the numerical solution of a nano-indentation on mono-crystalline silicon with a spherical indenter of 5 μm in radius. A quarter of a cubic sample of 5 μm in depth is considered. The size of the control volume is proper enough to eliminate any boundary effects, as can be seen in Fig. 3. The penetration is simulated by gradually applying an upward displacement on the control volume.
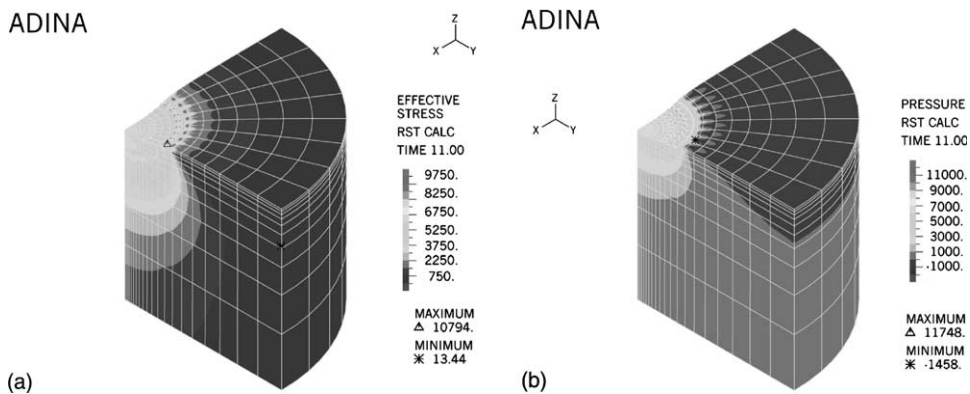

Fig. 3. Stress (MPa) at the penetration of 320 nm: (a) effective stress and (b) hydrostatic stress.

3.1. Onset of phase transformation

At a very small penetration the material is elastic. After that the first limiting surface is reached in a small volume of highly stressed material and silicon becomes elastic–plastic. At a penetration of about 100 nm, both the width and depth of the elastic–plastic zone become around 700 nm (Fig. 4a).

With increasing the penetration, the volume of the elastic–plastic silicon increases (Fig. 4b). Based on their molecular dynamics analysis, Zhang and Tanaka (1999) pointed out that the phase transformation in silicon is initiated by the octahedral shear stress, but is further facilitated by the hydrostatic pressure. The present mechanics analysis clearly confirms their conclusion. The first material points to transform are not the ones immediately under the indenter. At the indentation of 150 nm, a small volume of a depth of 40 nm and a width of 465 nm, with high deviatoric stresses but relatively low hydrostatic pressure, initiates the metamorphism to β-tin Si (Fig. 4b).
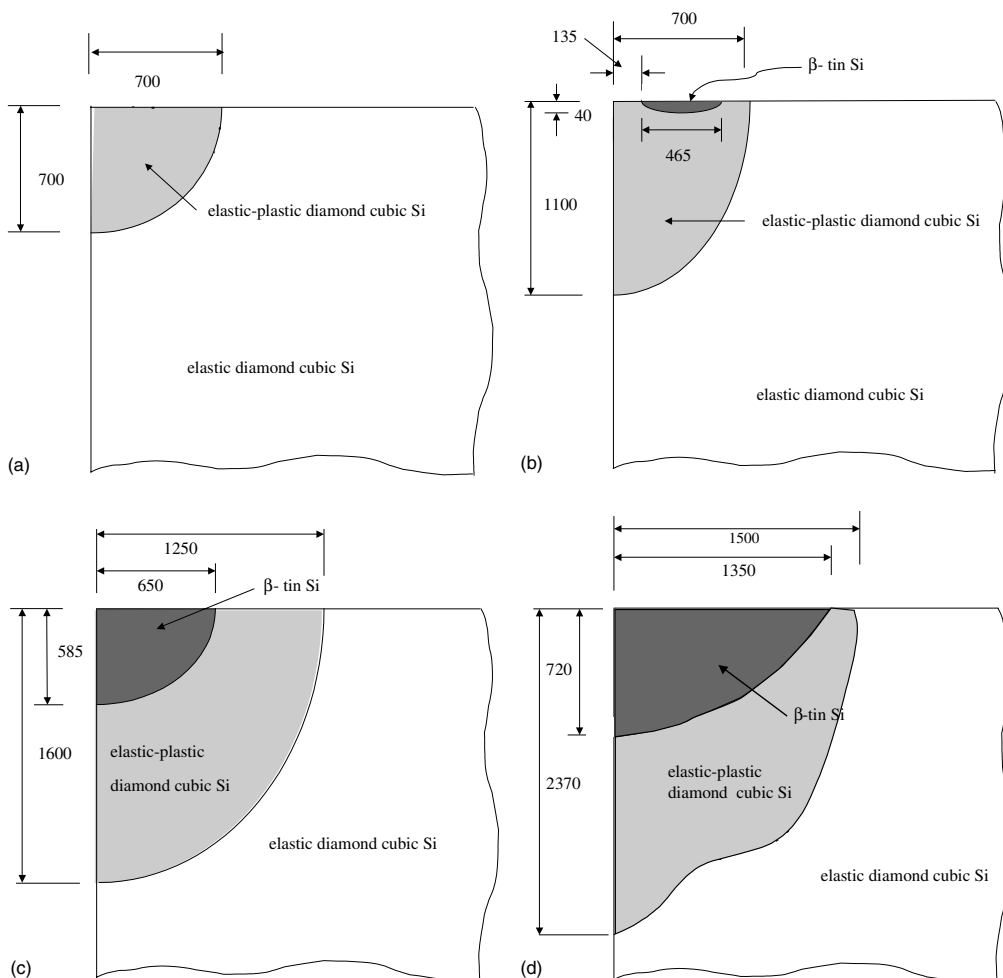

Fig. 4. Width and depth (nm) of the silicon phases at various penetrations of the indenter: (a) penetration = 100 nm, (b) penetration = 150 nm, (c) penetration = 200 nm and (d) penetration = 320 nm. (Note that to visualise the small zones of phase transformations, some boundaries are not exactly drawn in this figure.)

As the penetration increases further the volume of the new phase grows and at 200 nm a large volume of a depth of around 585 nm and a width of about 650 nm is already transformed (Fig. 4c). At the end of indentation, i.e., at 320 nm, an area as wide as 1.35 μm and as deep as 720 nm is occupied by Si II (Fig. 4d). While the width of 1.35 μm is close to the experimental width of 1.5 μm (Zarudi and Zhang, 1999), the depth of 720 nm is larger than the experimental observation of 420 nm. This may be caused by some uncertain factors in experimentation, e.g., the imperfections of the indenter's shape, its diameter and the number of the loading increments in the indentation tests.

3.2. Pop-in

The stress state in indentation is complex; both deviatoric and hydrostatic stress components exist and they are of comparable magnitudes. At the penetration of 320 nm, the hydrostatic stress does not exceed 7.4 GPa, and the maximum effective stress in the material is about 6.2 GPa. The highest hydrostatic pressure appears at the point immediately under the indenter, at which the magnitude of the effective stress is much lower (see Fig. 3a and b). Fig. 5a–e show the development of the stresses in loading and unloading at various depths under the indenter for material points along the axis of symmetry. The pattern is similar for points in other zones.

As mentioned above the phase transformation from Si I to Si II first occurs at the penetration of 150 nm, in a small volume on the surface outside the indenter-silicon contact interface (Fig. 4b). However, since the popping volume is small, the volumetric reduction is negligible and the load-penetration curve looks 'well-behaved'.

With the increase in loading, a larger volume of Si pops-in. At the penetration of 200 nm the new phase occupies a large volume in the deformation zone (Fig. 4c) where the effective stress is of the magnitude of 5.8–6.3 GPa, and the hydrostatic stress is within the range of 3–6.8 GPa. The volumetric change becomes more significant and at the penetration of 210 nm the load-penetration curve registers a change in slope, pop-in, caused by the stress relaxation in the transformed zone (Fig. 6).

It must be pointed out that the transformed material points have a similar level of effective stress while the level of hydrostatic pressure varies significantly. This seems to conclude once again that the phase transformation is caused by the deviatoric stresses and it happens at an effective stress of around 6 GPa, i.e. $\tau_0 = 2.8$ GPa. This value is lower than $\tau_0 = 4.6$ GPa found by Zhang and Tanaka (1999) using molecular dynamic analysis. The discrepancy may be explained with the fact that molecular dynamics simulations used a much faster indentation speed, which lead to an increased stiffness of the material. In addition, a scale effect exists because the molecular model was only $10 \times 10 \times 10$ (nm^3).

During pop-in from the penetration of 200–210 nm, the hydrostatic pressure drops by around 0.3–0.5 GPa, as shown in Fig. 5a–d. After the pop-in, it increases smoothly again. The effective stress in all the transformed elements does not drop throughout the transformation process and remains almost constant after the pop-in, though the indentation load further increases. In the regions that do not experience the transformation, the hydrostatic stress continuously increases in loading (Fig. 5e).

3.3. Pop-out

Upon depressurization the stress components decrease at the same pace up to the point of pop-out (Fig. 5a–d). It has been noticed in the experiment that at a penetration of around 200 nm a large finite displacements occurs without a change of the applied force (Fig. 6). According to the new constitutive theory, this corresponds to a sudden inelastic volumetric reduction of 80% of the total volumetric strain in all the transformed material points. This confirms the suggestion that the pop-out is caused by a sudden volumetric increase of the transformed material due to a new phase transformation in unloading.
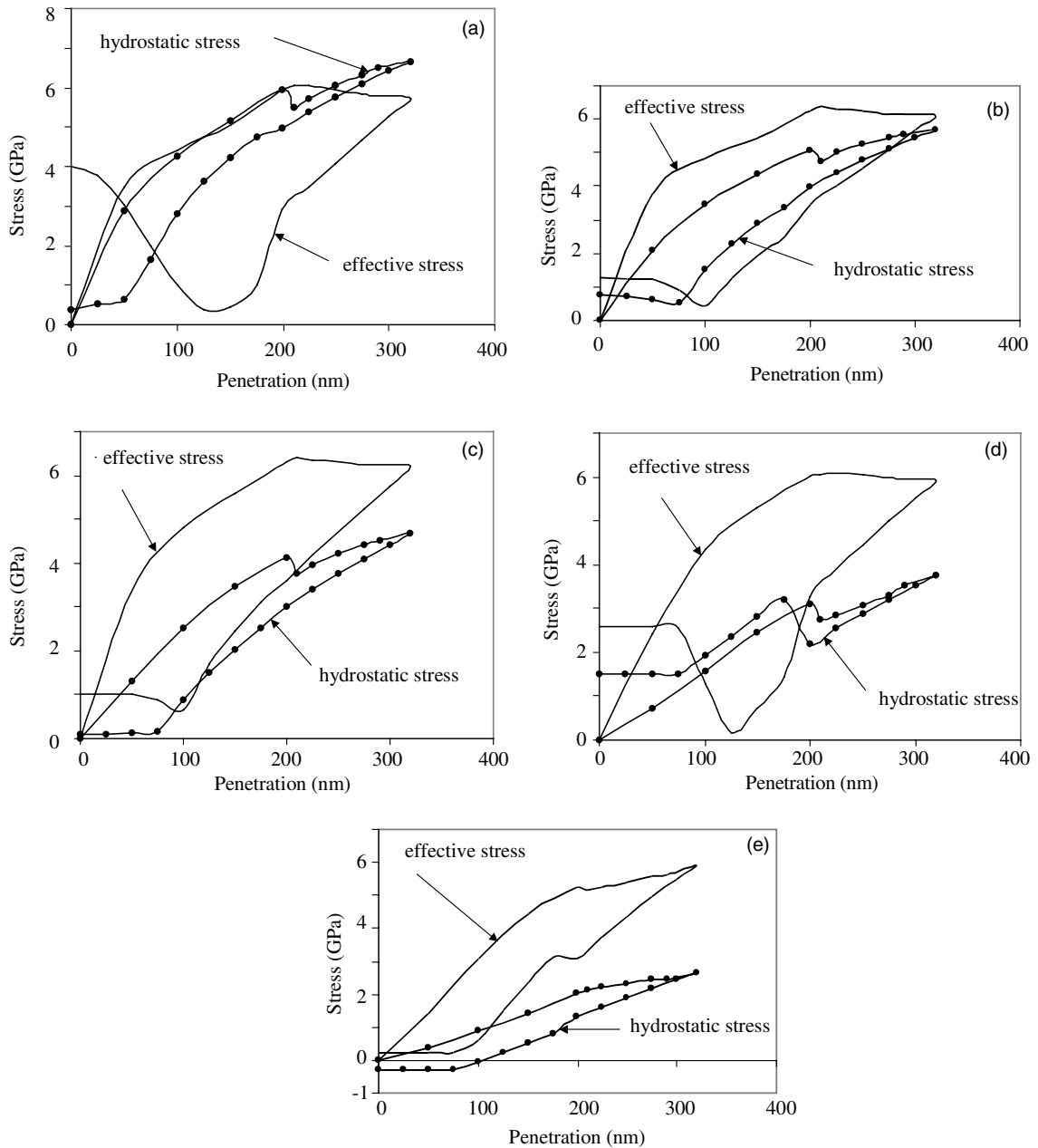
Fig. 5. Stresses $\bar{\sigma}$ and σ_m at various depths under the indenter along the axis of symmetry: (a) 100 nm, (b) 210 nm, (c) 360 nm, (d) 585 nm and (e) 890 nm.

An examination of the stresses in the transformed finite elements at the pop-out reveals that the effective stress in the transformed zone is mainly at the level of 3.5 GPa. In contrast, the hydrostatic stress varies largely from 6 to 2 GPa. This seems to suggest that the new phase transformation event at the pop-out is mainly due to the deviatoric stresses though influenced by the hydrostatic stress component.
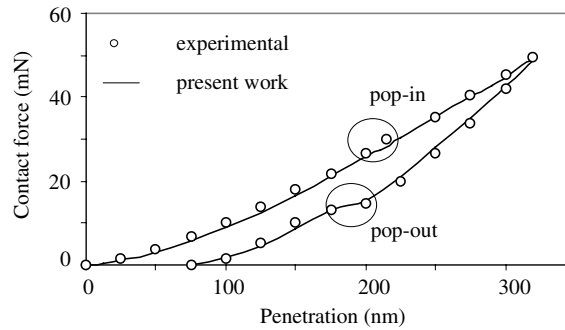
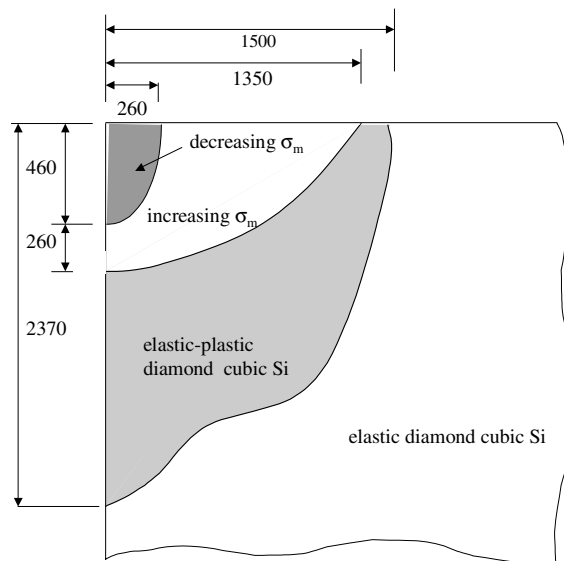Fig. 6. The load-penetration curve at the penetration of 320 nm.

Fig. 7. Zones of increasing/decreasing hydrostatic stress during the pop-out event (length unit: nm).

3.4. Secondary phase transformation

A different behaviour is observed at the pop-out at the interface between the transformed and un-transformed zone. The hydrostatic pressure there sharply increases from 2 to 3.1 GPa, while the effective stress decreases noticeably from 3 to 1.5 GPa (Figs. 5d and 7). This could be explained with the fact that this portion of the transformed volume becomes 'sandwiched' between the overlying expanding silicon and underlying diamond cubic Si, and is restrained from free expansion. As a result, the hydrostatic stress increases. If the stress level is sufficiently high, it can transform the material into a denser phase, bcc Si. In the FE simulations this 'secondary' phase transformation occurs in a volume of around 130 nm in depth and 300 nm in width (Fig. 8) at an effective stress of around 2 GPa and a hydrostatic stress of 3 GPa (Fig. 5d). The bcc silicon phase in unloading was experimentally found by Zarudi and Zhang (1999) at the bottom of the transformed zone. This is highly in agreement with the current prediction.
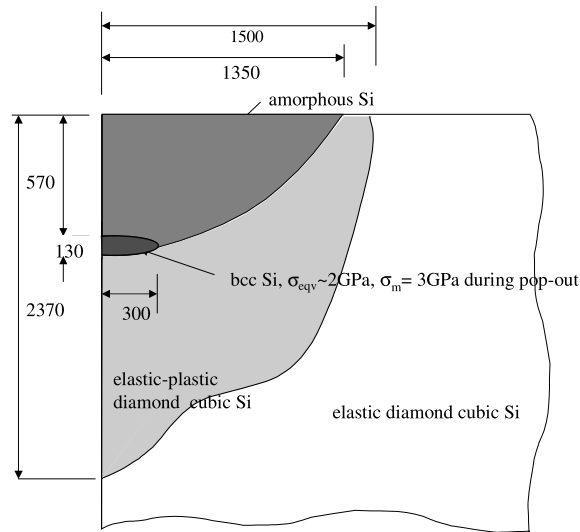
Fig. 8. The residual deformation zone in the substrate and the bcc-structured Si after complete unloading (length unit: nm).

3.5. Residual stresses and residual deformation

After the pop-out in unloading, the effective stress decreases up to an indentation of 100–150 nm and then increases to its residual value (Fig. 5a–d). The residual effective stress is higher at the points immediately under the indenter (3–4 GPa). At the interface between the transformed and untransformed Si, it is around 2.6 GPa. In the middle of the transformed zone, however, the residual effective stress is about 1.3 GPa only. On the other hand, the hydrostatic stress after the pop-out decreases smoothly to around 1.3 GPa at the points immediately under the indenter, and to around 1.5 GPa at the interface between the transformed and untransformed volume. In the middle zone the residual hydrostatic stress is about 0.1–0.4 GPa. Although the effective residual stresses increase in a large volume of the material, the stress level does not seem to be high enough to cause another phase transformation.

The depth of the residual mark upon complete unloading is found to be 75 nm in the FE simulations, which exactly matches the experimental measurement of Zarudi and Zhang (1999) (Fig. 6). However, the phase transformation zone and the elastic–plastic zone predicted theoretically appear deeper than the experimental ones.

4. Conclusions

An FEA simulation of nano-indentation of mono-crystalline silicon by a spherical indenter is performed using a new constitutive model recently developed. The present prediction describes the whole process of phase transformations in loading and unloading that is impossible in an experimental investigation. Moreover, the prediction fits closely the experimental findings of the load-penetration curve and the pop-in and pop-out events. The discontinuities in the load-penetration curve are found to be caused by the volumetric reduction/expansion of the material during the phase transformations. A band of a denser phase at the bottom of the deformation zone, the bcc silicon, was found to appear at an effective stress of around 3 GPa and hydrostatic pressure of around 2 GPa.

Equally importantly, the present study reveals that in indentation a material point in the deformation zone can experience a local unloading in the overall loading process, and similarly, it can undergo a local

loading in the overall unloading process. It is clear from the above discussions that these local loading and unloading events play an important role in the phase transformation processes.

Acknowledgements

References

ADINA, 1997. User-Supplied Options Manual. ADINA R&D, Inc.

Bever, M.B., Wert, C.A., 1990. Mechanical Behaviour of Materials. McGraw-Hill Company.

Callahan, D.L., Morris, J.C., 1992. The extent of phase transformation in silicon hardness indentation. Journal of Materials Research 7, 1614–1617.

Cheong, W.C., Zhang, L.C., 2000. Molecular dynamics simulations of phase transformations in silicon monocrystals due to nano-indentation. Nanotechnology 11, 1–7.

Duclos, S.J., Vohra, Y.K., Ruoff, A.L., 1990. Experimental study of the crystal stability and equation of state of Si to 248 GPa. Physical Review B 41, 012021–012028.

Gogotsi, Y.G., 2000. Cyclic nanoindentation and Raman microscopy study of phase transformations in semiconductors. Journal of Materials Research 15, 871–879.

Hanfland, M., Schwarz, U., Syassen, K., Takemura, K., 1999. Crystal structure of the high-pressure phase silicon VI. Physical Review Letters 82, 1197–1200.

Hu, J.Z., Merkle, L.D., Menoni, C.S., Spain, I.L., 1986. Crystal data for high-pressure phases of silicon. Physical Review B 34, 4679–4684.

Inamura, T., Takezawa, N., 1997. Brittle/ductile transition phenomena observed in computer simulations of machining defect-free monocrystalline silicon. Annals of the CIRP 46, 31–34.

Mann, A.B., van Heerden, D., 2000. Size-dependent phase transformations during point loading. Journal of Materials Research 15, 1754–1758.

McMahon, M.I., Nelmes, R.J., Wright, N.G., Allan, D.R., 1994. Pressure dependence of the *Imma* phase of silicon. Physical Review B 50, 739–743.

Pfrommer, B.G., Cote, M., Louie, S.G., Cohen, M.L., 1997. Ab initio study of silicon in the R8 phase. Physical Review B 56, 6662–6668.

Piltz, R.O., Maclean, J.R., Clark, S.J., Ackland, G.J., Hatton, P.D., Crain, J., 1995. Structure and properties of silicon XII: a complex tetrahedrally bonded phase. Physical Review B 52, 4072–4085.

Swain, M.V., 1998. Mechanical property characterization of small volumes of brittle materials with spherical tipped indenters. Material Science in Engineering A 253, 160–166.

Tolbert, S.H., Herold, A.B., Brus, L.E., Alivisatos, A.P., 1996. Pressure-induced structural transformations in Si nanocrystals. Physical Review Letters 76, 4384–4387.

Vodenitcharova, T., Zhang, L.C., submitted for publication. A new constitutive model for the phase transformations in mono-crystalline silicon.

Weppelmann, E.R., Field, J.S., Swain, M.V., 1993. Observations, analysis, and simulation of the hysteresis of silicon using ultra-micro-indentation with spherical indenters. Journal of Materials Research 8, 830–840.

Weppelmann, E.R., Field, J.S., Swain, M.V., 1995. Influence of spherical indentor radius on the indentation-induced transformation behaviour of silicon. Journal of Materials Science 30, 2455–2462.

Williams, J.S., Chen, Y., Wong-Leung, Kerr, A., 1999. Ultra-micro-indentation of silicon and compound semiconductors with spherical indenters. Journal of Materials Research 14, 2338–2343.

Wu, Y.Q., Yang, X.Y., Xu, Y.B., 1999. Cross-sectional electron microscopy observation on the amorphized indentation region in [0 0 1] single-crystal silicon. Acta Materialia 47, 2431–2436.

Yoshino, M., Aoki, T., Chandrasekaran, N., Shirakashi, T., Komanduri, R., 2001. Finite element simulation of plane strain plastic–elastic indentation on single-crystal silicon. International Journal of Mechanical Sciences 43, 313–333.

Zhang, L.C., Mahdi, M., 1996. The plastic behaviour of silicon subjected to micro-indentation. Journal of Materials Science 31, 5671–5676.

Zhang, L.C., Tanaka, H., 1999. On the mechanics and physics in the nano-indentaion of silicon monocrystals. JSME International Journal Series A 31, 546–559.

Zarudi, I., Zhang, L.C., 1999. Structure changes in mono-crystal silicon subjected to indentation-experimental findings. Tribology International 32, 701–712.